Journal of Radioanalytical and Nuclear Chemistry (2018) 317:1477–1483
https://doi.org/10.1007/s10967-018-6041-8

Optimization of Linac-based neutron source for thermal neutron activation analysis

Mona Zolfaghari[1] · S. Farhad Masoudi[1] · Faezeh Rahmani[1]

Received: 30 March 2018 / Published online: 1 August 2018

Abstract
A 20 MeV electron Linac based neutron beam has been shaped for neutron activation analysis (NAA) technique. A beam shaping assembly (BSA) has been simulated using MCNPX2.6 code to increase the thermal neutron flux and decrease the epithermal and fast neutrons as much as possible at the beam port for NAA facility. Final BSA containing 1.5 cm tungsten as photoneutron target, 7 cm BeD_2 and 4 cm polyethylen as moderators surrounded by BeO as reflector as well as 6 cm PE as collimator layer provides 1.67×10^{10} (n/cm^2 mA) at the beam port. The results of final configuration show that the proposed system leads to increasing of thermal to epithermal and thermal to fast neutron flux up to approximately 5.29, 6.22, respectively.

Keywords Electron linear accelerator · Neutron activation analysis · Photoneutron source · Beam shaping assembly

Introduction

Neutron Activation Analysis (NAA) is a powerful nondestructive, fast and precise technique [1–3] compared to the other methods for elemental analysis in materials [4–7]. This technique is extensively applied in industrial manufacturing, environmental evaluating and medical applications [1–3, 7, 8]. In this technique, the energy and intensity of the gamma rays emitted through thermal neutron capture reaction leads to identification of the majority of elements due to the large thermal neutron capture cross sections as well as determination of their concentrations [9].

Neutron sources utilized in analysis based on neutron activation are nuclear reactors, isotopic sources of ^{241}Am/Be and ^{252}Cf, accelerators and neutron generators based on deuterium–deuterium (D–D) and deuterium–tritium (D–T) fusion reactions [10, 11]. Among these neutron sources, electron linear accelerators (Linacs) can be considered as a favorable option to produce photoneutrons for medical and industrial applications such as NAA [12, 13].

For NAA technique based on the thermal neutron capture reaction, a high thermal neutron flux provided by a suitable NAA setup will be required. Therefore, the fast neutron sources must be surrounded by Beam Shaping Assembly (BSA) containing composite of materials (CM) with proper compositions and thicknesses to achieve maximum thermal neutron flux while minimum epithermal and fast neutron fluxes at the output beam.

The aim of this work is to design a thermal neutron activation analysis setup containing composite of materials to generate the maximum thermal neutron flux along with minimum epithermal and fast neutron fluxes and to satisfy the thermalization criteria at the output beam. Following this purpose, fast neutrons produced by 20 MeV electron Linac and a 1.5 cm tungsten photoneutron target, have been thermalized by using a CM with optimized thicknesses and compositions. To achieve the neutron spectrum with high thermal neutron flux and minimized non-thermal portion, some parameters have been defined as criteria following recent works [14, 15], and BSA has been proposed to satisfy these criteria. The Monte Carlo N-Particle (MCNPX2.6) transport code has been used for optimization process. It is noted that all simulations in this work have been performed with ($< 5 \times 10^{-3}$) relative error and calculated by the F2 tally in energy bins: thermal ($< 10^{-6}$ MeV), epithermal (10^{-6}–10^{-2} MeV) and fast (up

✉ S. Farhad Masoudi
masoudi@kntu.ac.ir

[1] Department of Physics, K.N. Toosi University of Technology, P.O. Box 15875-4416, Tehran, Iran

to 20 MeV) neutrons, as well as, using cross sections from ENDF/B-VI Release 8 Photoatomic Data (mcplib) and Photonuclear Data from ENDF7u library.

Materials and methods

Electron–photoneutron source

Neutron producing based on electron–photon and photoneutron process is related to (e, γ) and (γ, n) reactions, respectively. Electrons emitted from Linac impinge on the target and lose their kinetic energy due to the effect of electric field of the target nucleus. Following this process, continuous X-ray spectrum or bremsstrahlung radiation will be produced [16]. Photoneutron reaction occurs when the energy of the incident photons is higher than the threshold energy of the (γ, n) reaction. The threshold energy is variable in different target. It is 7–8 and 16–18 MeV for high-Z materials (W, Pb, Fe) and low-Z elements (C, O), respectively, except for Be and D (1.67 and 2.23 MeV, respectively) [17]. On the other hand, high-Z materials have larger (γ, n) cross sections than those of light elements. The photoneutron energy is calculated as follow [18]:

$$E_n = \frac{M-1}{M}\left[E_\gamma - E_{\text{th}} - \frac{E_\gamma^2}{2m_nc^2(M-1)}\right] + E_\gamma\left[\frac{2(M-1)(E_\gamma - E_{\text{th}})}{m_nc^2M^3}\right]^{1/2}\cos\theta \quad (1)$$

where M is the atomic mass number of target, E_γ is the photon energy (MeV), E_{th} is the (γ, n) reaction threshold (MeV) and θ is the angle between incident photon and neutron emission direction. According to the second part of this equation, by increasing atomic mass number of target, E_n varies slowly, therefore, the first part will be effective for large atomic mass number.

Here, a 20 MeV electron linear accelerator has been considered as an electron source. The electron–photon and photoneutron targets have been considered due to their high atomic number, low (γ, n) reaction threshold energy and high (γ, n) cross section.

Design of beam shaping assembly

To thermalize the fast neutrons emitted from photoneutron source and to obtain maximum thermal neutron flux at the beam port, a set of CM, containing moderator, reflector and collimator with different thicknesses and radiuses in cylindrical shape have been considered around the neutron source. Following some recent works [14, 15], the criterion K has been considered as the CM thermalization efficiency, $K = \Phi_{\text{th}}^2/\Phi_{\text{total}}$ (n/cm^2 mA), where Φ_{th} is the thermal neutron flux and Φ_{total} is the total neutron flux at the beam port. As our optimization process is based on having maximum thermal neutron flux, while minimum epithermal and fast neutrons, the greater value of K means the better neutron beam is provided for NAA application.

In addition, to achieve the highest thermal neutron flux while minimum epithermal and fast neutron fluxes as much as possible, the following completed criteria have been defined [15]: $C_2 = \Phi_{\text{th}}/\Phi_{\text{epi}}$, $C_3 = \Phi_{\text{th}}/\Phi_{\text{fast}}$ and $C_4 = \Phi_{\text{th}}/\Phi_{(\text{epi}+\text{fast})}$, where Φ_{fast} and Φ_{epi} are the fast and epithermal neutron flux at the beam port, respectively.

Results and discussion

Electron beam produced by Linac head with 20 MeV energy impinges on center of an electron–photon and photoneutron target after passing through a cylindrical air hole with 5 mm in radius and 40 cm in thickness. For electron–photon and photoneutron target, following previous works [19], tungsten (W) in spherical shape has been selected as a proper (e, γ) and (γ, n) converter. Tungsten

Table 1 The properties of materials utilized in simulations as air, electron–photon and photoneutron target, moderators, reflector and collimators

Materials	Density (g/cm^3)	Isotopes (%)
Air	0.001293	^{14}N (75.52), ^{16}O (23.18), ^{1}H (14.37), ^{40}Ar (1.29)
Tungesten (W)	19.254	^{182}W (26.16), ^{183}W (14.20), ^{184}W (30.58), ^{186}W (28.95)
Polyethylen (PE)	0.9581	^{12}C (85.63), ^{1}H (14.37)
Beryllium oxide (BeO)	3.01	^{9}Be (36.04), ^{16}O (63.94)
Beryllium deutrium (BeD_2)	0.765	^{9}Be (66.00), ^{2}D (34.00)
Teflon (CF_2)	2.25	^{19}F (76.00), ^{12}C (24.00)
Heavy water (D_2O)	1.11	^{2}D (20.00), ^{16}O (80.00)
Aluminum oxide (Al_2O_3)	3.96	^{16}O (28.32), ^{27}Al (71.67)
Fluental	3.00	^{27}Al (52.18), ^{19}F (47.56), ^{7}Li (0.26)
Graphite	2.267	^{12}C (100)
Plexiglas	1.18	^{12}C (59.99), ^{16}O (31.96), ^{1}H (8.05)

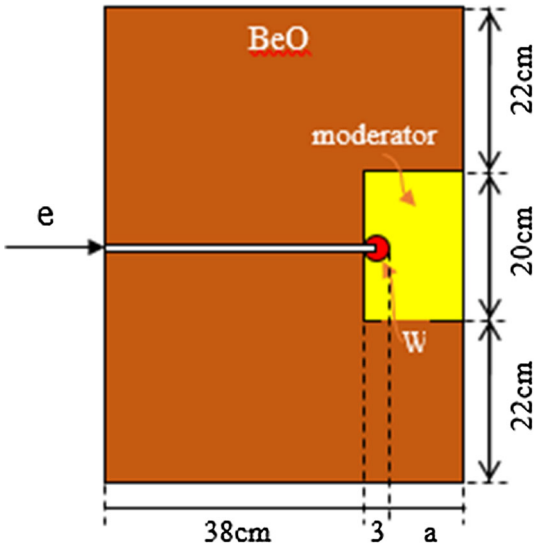

Fig. 1 Schematic view of initial Beam Shaping Assembly contacting cylindrical moderators, reflector as well as spherical electron–photon and photoneutron target

has high atomic number, (γ, n) reaction threshold energy about 6–8 MeV and high (γ, n) cross section (about 400–700 mb) [20]. In addition to the material, its thickness is also of high importance in neutron yield. While tungsten with the optimized radius of 6 cm has been selected as a photoneutron target in BNCT [19], it would not optimized for other purposes, e.g. NAA. It is due to the different criteria recommended for each application. Optimizing the radius of tungsten is therefore vital in this work.

The optimized radius has been chosen through a large number of simulations for criterion K corresponding to different thicknesses of materials mentioned in Table 1 surronded the spherical tungesten (see Fig. 1 as the schematic view of initial beam shaping assembly). Some of the obtained results are shown in Fig. 2. In all simulations, BeO has been selected as the most appropriate reflector considering the results of a set of simulations in our previous works. According to the results, the radius of 1.5 cm tungesten leads to the maximum value of K. Also, the optimized radius and thickness of BeO in cylindrical shape have been obtained 32 cm and (41 + a) cm, respectively. The 'a' thickness is variable due to different thicknesses of moderators employed around and in front of Was shown in Fig. 1.

In order to meet the higher values of criterion K, using materials as moderators in BSA has been proposed. This cell in cylindrical shape surrounds around of W and in front of it. Different thicknesses of this cell ('a' in Fig. 1) have been tested for better value of K. The results can be seen in Fig. 3.

Obviously, PE, Plexiglas, BeD_2 and D_2O lead to the higher values of K compared to others. It can be justified

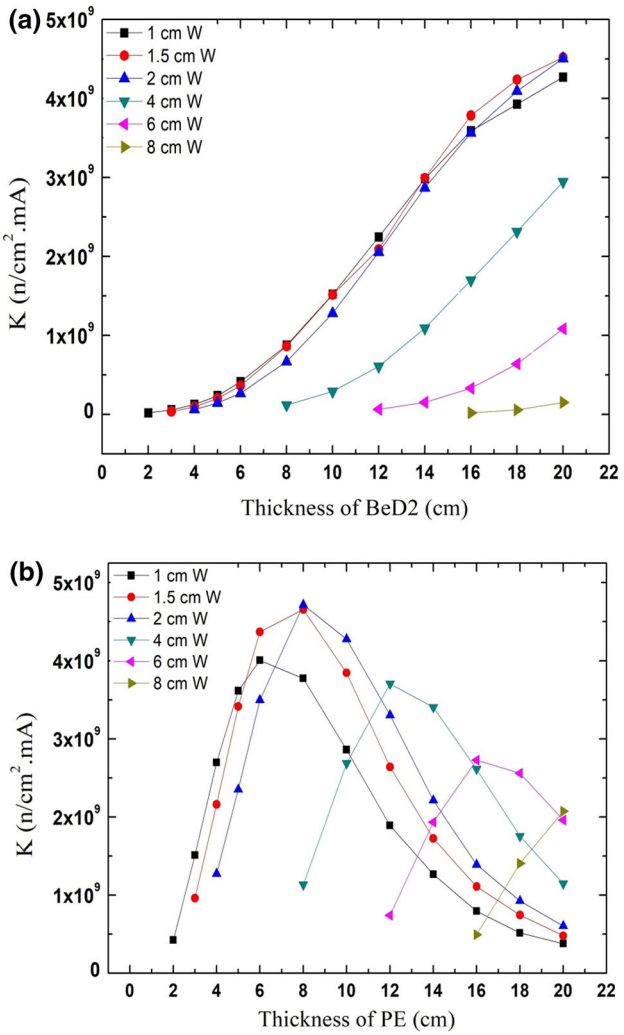

Fig. 2 The criterion K for different radius of W surrounded by (**a**) BeD_2 and (**b**) PE. The horizental axis is the thickness of BeD_2 and PE around and in front of W

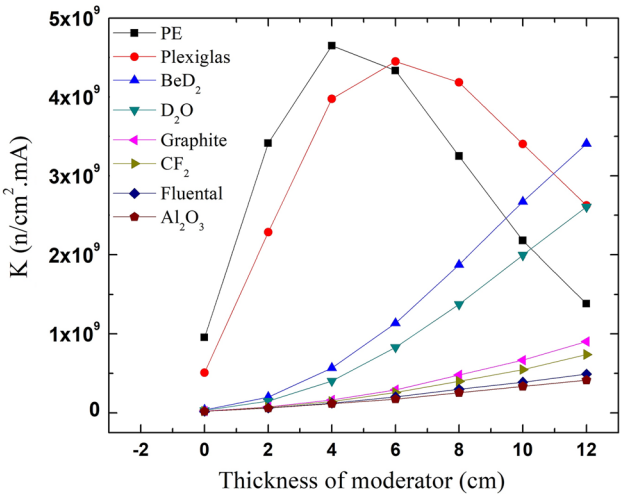

Fig. 3 Criterion K for different materials as moderators in Fig. 1

Table 2 The criterion K ($\times 10^9$) for PE, Plexiglas, BeD_2 and D_2O as the first and the second moderator in front of W in columns and rows, respectively

	PE (2 cm)	PE (4 cm)	PE (6 cm)	PE (8 cm)	PL (2 cm)	PL (4 cm)	PL (6 cm)	PL (8 cm)	BeD_2 (2 cm)	BeD_2 (4 cm)	BeD_2 (6 cm)	BeD_2 (8 cm)	D_2O (2 cm)	D_2O (4 cm)	D_2O (6 cm)	D_2O (8 cm)
PE (2 cm)	4.65	4.33	3.25	2.18	4.53	4.61	3.94	3.10	3.95	4.10	3.90	3.76	4.04	4.06	4.09	3.94
PE (4 cm)	4.33	3.25	2.18	1.38	4.54	3.70	2.89	2.17	4.56	3.99	3.68	3.27	4.53	4.28	3.96	3.58
PE (6 cm)	3.25	2.18	1.38	0.88	3.57	2.68	1.94	1.48	3.73	3.17	2.77	2.38	3.85	3.43	3.07	2.73
PE (8 cm)	2.18	1.38	0.88	0.59	2.46	1.85	1.26	0.94	2.57	2.12	1.85	1.63	2.75	2.39	2.06	1.86
PL (2 cm)	4.32	4.53	3.62	2.49	3.98	4.45	4.19	3.40	3.16	3.48	3.62	3.65	3.02	3.43	3.64	3.67
PL (4 cm)	4.52	3.84	2.75	1.82	4.45	4.19	3.40	2.63	4.21	4.13	3.99	3.61	4.32	4.25	4.21	3.95
PL (6 cm)	3.96	2.93	1.92	1.24	4.19	3.40	2.63	1.97	4.22	3.85	3.46	3.12	4.40	4.07	3.77	3.50
PL (8 cm)	3.09	2.19	1.39	0.89	3.40	2.63	1.96	1.42	3.71	3.22	2.75	2.46	3.79	3.44	3.18	2.80
BeD_2 (2 cm)	3.08	5.58	5.23	3.78	1.99	4.60	5.51	4.94	0.56	1.14	1.88	2.67	0.52	1.01	1.63	2.29
BeD_2 (4 cm)	3.96	5.82	4.92	3.40	2.88	5.19	5.54	4.70	1.14	1.88	2.67	3.41	1.10	1.78	2.40	3.14
BeD_2 (6 cm)	4.65	5.75	4.50	3.05	3.77	5.45	5.50	4.37	1.88	2.67	3.41	4.08	1.84	2.53	3.25	3.89
BeD_2 (8 cm)	5.07	5.53	4.07	2.74	4.37	5.64	5.18	4.07	2.67	3.41	4.08	4.34	2.65	3.32	3.93	4.35
D_2O (2 cm)	2.67	5.23	4.99	3.60	1.65	4.16	5.12	4.73	0.43	0.95	1.64	2.32	0.40	0.83	1.37	2.00
D_2O (4 cm)	3.40	5.35	4.57	3.24	2.38	4.73	5.15	4.44	0.87	1.52	2.30	2.97	0.83	1.37	2.00	2.61
D_2O (6 cm)	3.93	5.24	4.28	2.87	2.99	4.87	5.00	4.15	1.42	2.14	2.86	3.43	1.37	2.00	2.61	3.22
D_2O (8 cm)	4.37	5.10	3.86	2.50	3.61	5.05	4.76	3.79	2.05	2.73	3.38	3.84	2.00	2.61	3.21	3.71

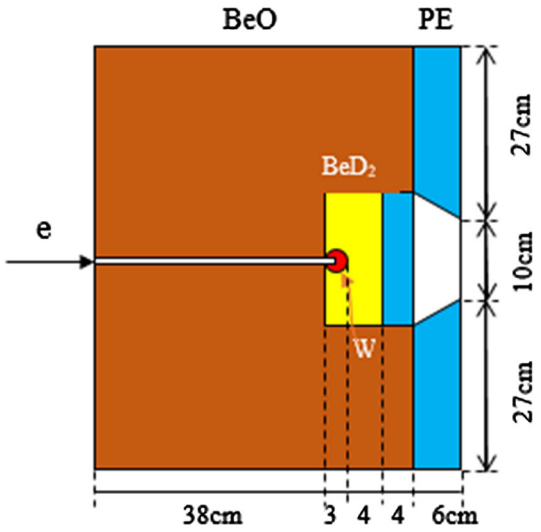

Fig. 4 The final BSA as the optimized configuration

considering the high elastic scattering cross section in the region of fast and epithermal energies (> 1 barn) for these materials, and low thermal neutron capture cross section ($< 10^{-2}$ barn) as well.

Although the results exhibit that maximum value of the criterion K corresponds to PE with 4 cm thickness, however different arrangements of the four mentioned materials as the first and the second moderator have been tested.

The results, reported in Table 2, show that 4 cm of BeD_2 (a = 4 cm in Fig. 1) followed by 4 cm PE provides the maximum value of K. It is due to the lower photoneutron threshold energy of Be (1.67 MeV) and D (2.23 MeV). Therefore, the second moderator, PE, shifts-down the energy of fast and epithermal neutrons produced from BeD_2 in (γ, n) reaction, according to Eq. 1. Thermal neutron flux, C_2, C_3 and C_4 for this optimized configuration

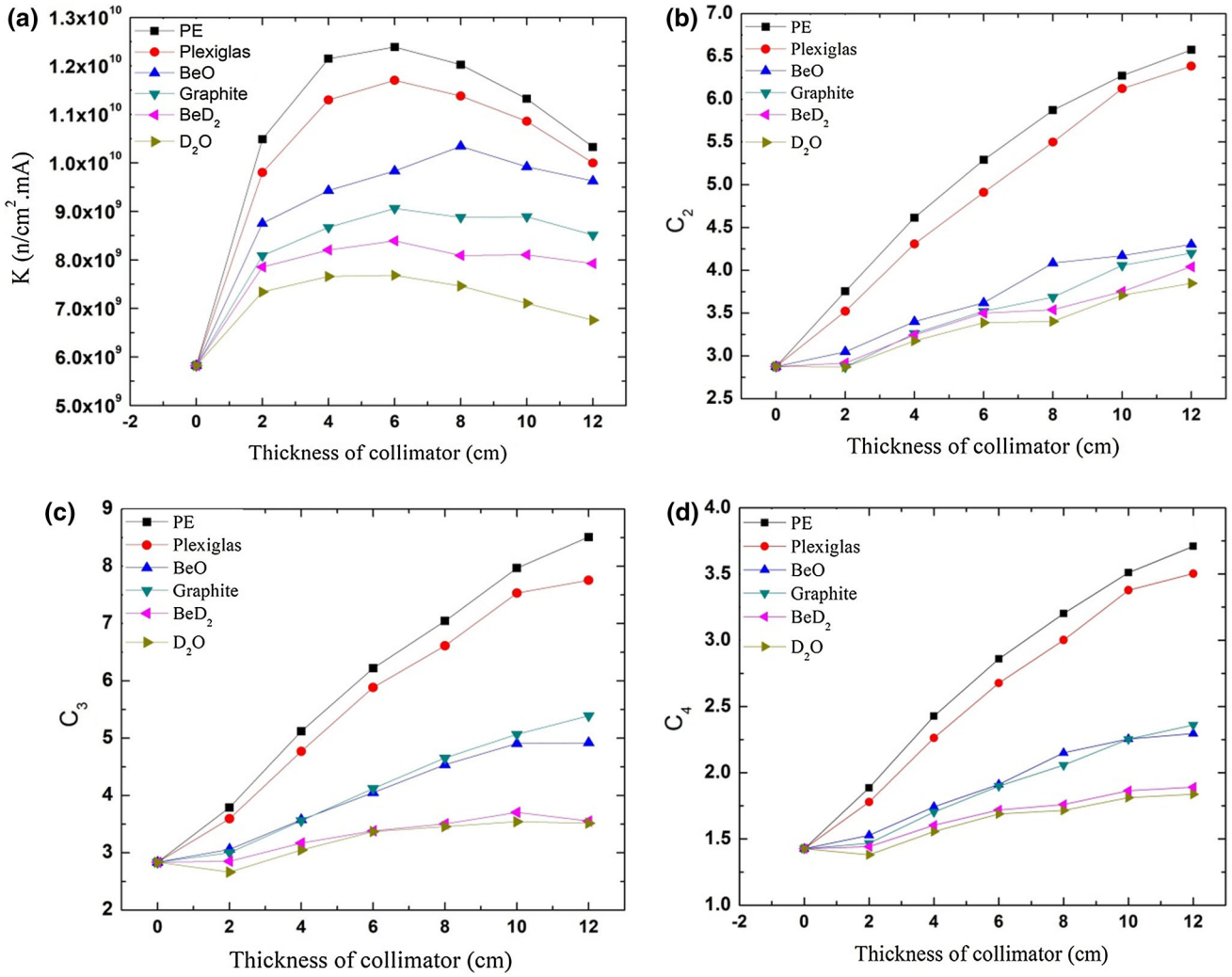

Fig. 5 The criteria (**a**) K, (**b**) C_2, (**c**) C_3 and (**d**) C_4 as a function of different thicknesses of collimators in front of the optimized BSA

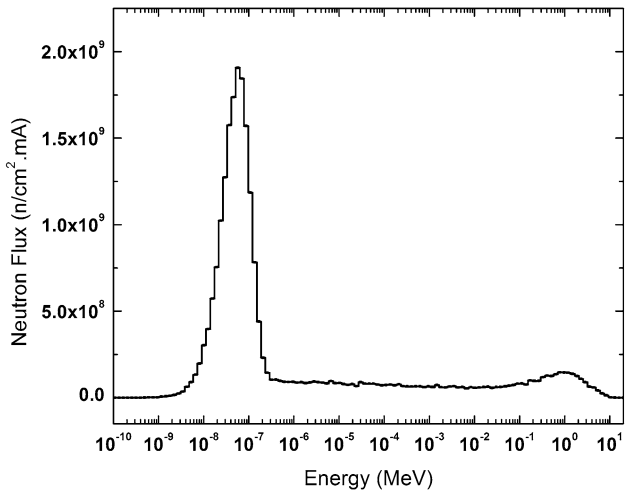

Fig. 6 Neutron spectrum at the output beam of the final BSA

Table 3 Comparing the criteria K, C_2, C_3 and C_4 of the final BSA with those of publised work [15]

	K	C_2	C_3	C_4
In this paper	1.24×10^{10}	5.29	6.22	2.86
[15]	3.21×10^{10}	2.89	2.75	1.41

It is noted that the unit of the criterion K in this paper is n/cm^2 mA while in publised work it is n/cm^2 s by considerring the maximum value of D–T neutron generator power (10^{15} (n/s)) [15]

is 9.90×10^9 (n/cm^2 mA), 2.88, 2.83 and 1.43, respectively.

To remove the remained epithermal and fast neutrons as much as possible, which simultaneously increases the values of the criteria K, C_2, C_3 and C_4 at the beam port, a collimator has been employed surrounding the conical cell containing air in front of the optimized CM, as shown in Fig. 4. The results at the beam port of such configuration with 10 cm in diameter for different thicknesses of collimator are presented in Fig. 5. According to these results, the maximum value of the criterion K is 1.24×10^{10} (n/cm^2 mA) which corresponds to 6 cm of PE. Also, the values of the criteria C_2, C_3 and C_4, as well as the thermal neutron flux for the final configuration (See Fig. 4) are 5.29, 6.22, 2.86 and 1.67×10^{10} (n/cm^2 mA), respectively. The neutron spectrum at the output beam has been shown in Fig. 6.

The mentioned criteria for the final BSA are reported in Table 3. Moreover, this Table compares the results of the criteria with those of the publised work for a configuration designed based on a D–T neutron generator [15]. Also, the comparition with recent published works will devote to design NAA systems to generate high thermal neutron fluxes based on reactor and D–D neutron generator which met the values of $3–5 \times 10^7$ (n/cm^2 s) [21] and 3.08×10^6 (n/cm^2 s) [7], respectively. The beam designed in the present work, not only satisfies the thermalization criteria corresponding to the final simulated BSA, but also produces high thermal neutron flux of 1.67×10^{10} n/cm^2 mA. According to the results, the final BSA with a 20 MeV electron linear accelerator exhibits the potential to be used for NAA.

Conclusions

The purpose of this simulation study was to design a thermal neutron activation analysis setup to produce the maximum thermal neutron flux along with minimum epithermal and fast neutron contribution for use in NAA technique. The neutron beam has been designed based on a 20 MeV Linac irradiated on tungsten as both electron and photoneutron target. A set of CM have been proposed to thermalize the initial fast neutrons emitted from the tungsten target. The simulated configurations have been assessed with K, C_2, C_3 and C_4 as thermalization criteria. The optimized BSA includes a tungsten sphere with 1.5 cm in radius as photoneutron target as well as 7 cm of BeD_2 and 4 cm of PE as moderators surrounded by 49 cm of BeO as reflector. This design has been accomplished with 6 cm of PE as the beam collimator which concurrently improves the calculated values for the thermalization criteria. The beam corresponding to the final configuration generates thermal neutron flux of 1.67×10^{10} (n/cm^2 mA). Moreover, K, C_2, C_3 and C_4 have been estimated about 1.24×10^{10} (n/cm^2 mA), 5.29, 6.22 and 2.86, respectively. Due to the high thermal neutron flux and satisfying the thermalization criteria, the final configuration shows the potential to be an appropriate candidate for NAA.

References

1. Naqvi AA, Garwan MA, Nagadi MM, Maslehuddin M, Al-Amoudi OSB, Rehman K (2009) Non-destructive analysis of chlorine in fly ash cement concrete. Nucl Instrum Methods Phys Res Sec A. 607(2):446–450
2. Udupi A, Panikkath P, Sarkar PK (2017) Photo-peak area ratios for estimation of elemental concentration in aqueous solutions using prompt gamma measurements. Appl Radiat Isot 128:6–12
3. Zhang Y, Jia WB, Gardner R, Shan Q, Hei D (2018) Study on the PGNAA measurement of heavy metals in aqueous solution by the Monte Carlo–Library Least-Squares (MCLLS) approach. Appl Radiat Isot 132:13–17
4. Wang XS (2013) Magnetic properties and heavy metal pollution of soils in the vicinity of a cement plant. J Appl Geophys 98:73–78

5. Du J, Jiang L, Shao Q, Liu X, Marks RS, Ma J, Chen X (2013) Colorimetric detection of mercury ions based on plasmonic nanoparticles. Small 9:1467–1481
6. West M, Ellis AT, Potts PJ, Streli C, Vanhoof C, Wobrauschek P (2015) 2015 Atomic Spectrometry Update–a review of advances in X-ray fluorescence spectrometry and their applications. J Anal At Spectrom 30:1839–1889
7. Zhang Z, Chong Y, Chen X, Jin C, Lijun Yang, Liu T (2015) PGNAA system preliminary design and measurement of In-Hospital Neutron Irradiator for boron concentration measurement. Appl Radiat Isot 106:161–165
8. Naqvi AA, Al-Matouq FA, Khiari FZ, Gondal MA, Isab AA (2013) Optimization of a prompt gamma setup for analysis of environmental samples. J Radioanal Nucl Chem 296(1):215–221
9. Lindstrom RM, Révay Z (2004) In Handbook of prompt gamma activation analysis: Beams and facilities. Springer, New York, pp 31–58
10. Canion B, Landsberger S (2013) Determining trace amounts of nickel in plant samples by neutron activation analysis. J Radioanal Nucl Chem 296:315–317
11. Moghaddam YR, Motavalli LR, Miri-Hakimabad HM (2013) Shielding optimization in an in vivo activation analysis setup. J Radioanal Nucl Chem 295:157–162
12. Mbarek R, Brahim A, Jallouli H, Trabelsi A (2013) Design of a photoneutron source based on a 10 MeV CIRCE III electron linac. Int J Adv Engin Technol 6:498–503
13. Rahmani F, Seifi S, Anbaran HT, Ghasemi F (2015) Design of photon converter and photoneutron target for high power electron accelerator based BNCT. Appl Radiat Isot 106:45–48
14. Uhlár R, Alexa P, Pištora J (2013) A system of materials composition and geometry arrangement for fast neutron beam thermalization: an MCNP study. Nucl Instrum Methods Phys Res Sec B 298:81–85
15. Uhlár R, Kadulová M, Alexa P, Pistora J (2014) A new reflector structure for facility thermalizing D-T neutrons. J Radioanal Nucl Chem 300(2):809–818
16. Burlon AA, Kreiner AJ, Valda AA, Minsky DM, Somacal HR, Debray ME, Stoliar P (2005) Optimization of a neutron production target and a beam shaping assembly based on the 7Li(p, n)7Be reaction for BNCT. Nucl Instrum Methods Phys Res Sec B. 229:144–156
17. Ongaro C, Zanini A, Nastasi U, Ródenas J, Ottaviano G, Manfredotti C, Burn KW (2000) Analysis of photoneutron spectra produced in medical accelerators. PhysMed Biol 45:L55–L61
18. Petwal VC, Senecha VK, Subbaiah KV, Soni HC, Kotaiah S (2007) Optimization studies of photo-neutron production in high-Z metallic targets using high energy electron beam for ADS and transmutation. Pramana J Phys 68:235–241
19. Masoudi SF, Rasouli FS (2015) Investigating a multi-purpose target for electron linac based photoneutron sources for BNCT of deep-seated tumors. Nucl Instrum Methods Phys Res Sec B 356–357:146–153
20. Chadwick MB, Oblozinsky P, Blokhin AI, Fukahori T, Han Y, Lee YO, Martins MN, Mughabghab SF, Varlamov VV, Yu B, Zhang J (2000) Handbook on photonuclear data for applications: cross sections and spectra. IAEA TECH-DOC, 1178
21. Vainionpaa HJ, Chen XA, Piestrup AM, Gary KC, Jones G, Pantell HR (2015) Development of high flux thermal neutron generator for neutron activation analysis. Nucl Instrum Methods Phys Res Sec B. 350:88–93